Electrochimica Acta 515 (2025) 145709

Contents lists available at ScienceDirect

Electrochimica Acta

journal homepage: www.journals.elsevier.com/electrochimica-acta

Study of surface-active substances using alternating current voltammetry and mercury electrode by potentiostat without phase sensitivity modules

Kristijan Vidović [a,b,*], Niki Simonović [b], Nikola Tasić [a], Samo B. Hočevar [a], Irena Ciglenečki [b]

[a] National Institute of Chemistry, Department of Analytical Chemistry, Hajdrihova 19, 1000 Ljubljana, Slovenia
[b] Ruđer Bošković Institute, Division for Marine and Environmental Research, Laboratory for Physical Oceanography and Chemistry of Aquatic Systems, Bijenička cesta 54, 10000 Zagreb, Croatia

ARTICLE INFO

Keywords:
AC voltammetry
single-frequency EIS
SAS
faradaic and non-faradaic impedance
environmental samples

ABSTRACT

Pursuing an effective and sensitive methodology for studying surface-active substances (SAS) remains a major challenge and continues to attract significant attention. Here, we propose and evaluate an electrochemical methodology that utilizes alternative current (AC) voltammetry in combination with contemporary potentiostats without an integrated lock-in amplifier. The proposed methodology effectively separates capacitive currents from faradaic currents and is compared to phase-sensitive AC voltammetry (PSACV), which is conventionally used to assess SAS. The practical applicability of this methodology is demonstrated by measuring SAS in real samples with complex matrices, such as seawater and atmospheric aerosol water extracts. Furthermore, the proposed methodology opens vast possibilities for its application in environmental sciences, where SAS play an important role.

1. Introduction

Since its discovery in the early 1950s, AC voltammetry has shown great potential in faradaic and non-faradaic electroanalysis [1–5]. AC voltammetry superimposes the alternating voltage to a DC potential ramp. It can be considered a single-frequency impedimetric method, where the total impedance of the cell is measured through the device impedance bridge by adjusting the real ohmic resistance (R) and the imaginary capacitance (X_c) in the opposite arm of the bridge. In such a system, the values of real ($Z' = R$) and imaginary ($Z'' = X_c = 1/j\omega C$) impedance connected in a series at a given frequency can be determined.

AC voltammetry aims to measure the AC that flows due to the oxidation–reduction (faradaic process) and adsorption-desorption (non-faradaic) processes. The total measured series impedance in the electrochemical cell can be split into faradaic and non-faradaic impedance. A corresponding Randles circuit ($R_S(Z_FC_{dl})$) can represent this physicochemical process, where faradaic impedance (Z_F) and double-layer charging capacity (C_{dl}) are in parallel and in series with the solution resistance (R_S). The C_{dl} element is related to the non-faradaic process, while the Z_F element corresponds to the charge transfer, which is a faradaic process [2,6–8].

In the past, the sensitivity of AC voltammetry, with respect to the faradaic processes, was limited mainly by the presence of the charging current (non-faradaic processes). This limitation is intrinsic because the proposed Randles circuit leads to the AC output value, with its magnitude determined by the total impedance of the whole circuit, including faradaic and non-faradaic processes. The observed AC output value will represent faradaic processes only when the faradaic impedance is significantly smaller than the capacitance. Such a case can be met at lower frequencies of AC voltage, where the capacitor exhibits a very high impedance (capacitance), and hence, AC passes mainly through the parallel resistor, corresponding to the faradaic impedance; thus, the imaginary impedance component becomes negligible in this case [9–12]. However, to overcome the sensitivity problem caused by charging current, different electronic modules have been developed; the most successful were those incorporating sinusoidal alternating voltage phase sensitivity modules [2,6]. Lock-in amplifiers are modules that detect and measure very small AC signals; they are frequency and phase-selective amplifiers. Their effectiveness is determined by how well they amplify an AC signal of a particular frequency and phase while minimizing other signals. Initially, the main goal of introducing lock-in amplifiers in AC voltammetry was to improve the detection limits of the faradaic processes [13–15].

Although the faradaic and non-faradaic (capacitive) currents are

* Corresponding author: Department of Analytical Chemistry, National Institute of Chemistry, Hajdrihova 19, SI, 1000 Ljubljana, Slovenia.
E-mail address: kristijan.vidovic@ki.si (K. Vidović).

https://doi.org/10.1016/j.electacta.2025.145709
Received 28 October 2024; Received in revised form 14 January 2025; Accepted 14 January 2025
Available online 17 January 2025

additive, these two currents are not in phase. The capacitive current has a phase angle of 90° with respect to the AC voltage, the same as in any conventional AC capacitor [6]. On the other hand, the faradaic current is represented by a resistor with a phase angle of 0°, which means that the voltage and current are in phase. Therefore, the frequency of the non-faradaic and faradaic currents can be identical, but their phase angles with respect to the applied AC voltage are different. Thus, the lock-in amplifier selectively measures the faradaic or non-faradaic current [16,17]. Lock-in amplifiers suppress only the signal that is not of interest. They are often employed to suppress the non-faradaic signal, enabling the detection limits as low as 1×10^{-7} M for electrochemically reversible redox species [18]. On the other hand, another advantage of utilizing a lock-in amplifier is that it is also possible to selectively measure the non-faradaic current, i.e., capacitive current.

In the case of the mercury (Hg) electrode, having an ideally homogeneous surface where an ideal capacitor can represent the interface between the working electrode and the solution, adsorption-desorption processes (expressed through non-faradaic current) can be precisely measured both qualitatively and quantitatively. From this point of view, a new branch of electrochemistry called tensammetry was developed and centered around PSACV [2,19–21]. With the recent development of other voltammetric methods, particularly square-wave voltammetry (SWV) [22] (the limits of detection reaching 10^{-10} M without an amplifier), conventional AC voltammetry fell into oblivion. Only a few electrochemical groups still employ PSACV, with a notable presence in Eastern European countries that have been historically linked to the usage of Hg electrodes [23,24].

Due to reduced demand for out-of-phase measurements (PSACV) and the satisfactory detection limits of SWV, along with the emergence of more advanced non-electrochemical methodologies, manufacturers of electrochemical equipment have ceased the production of potentiostats with phase sensitivity modules. While the latest models of potentiostats allow AC voltammetry, there is usually no option to define the angle between current and voltage simply because these instruments lack an integrated lock-in amplifier. Such potentiostats measure only the total impedance, implying that the AC output value is a sum of faradaic and non-faradaic currents.

Motivated by these challenges, the main objective of this study is to evaluate the feasibility of using total impedance as an output signal in AC voltammetry. The proposed methodology aims to identify and quantify adsorption-desorption processes on the surface of the Hg electrode. Considering the potential use of the method in several applications ranging from environmental protection, energy storage, and medical diagnostics to materials science, we believe that optimizing and validating AC voltammetric measurements of SAS using potentiostats without phase sensitivity modules is highly important. Therefore, the proposed methodology simplifies complex techniques such as electrochemical impedance spectroscopy (EIS) and compares them to the conventional PSACV.

2. Materials and methods

AC voltammetric measurements were performed on two types of potentiostats: (i) the new-generation potentiostat without an integrated lock-in amplifier (Autolab PGSTST204, Metrohm) and (ii) the potentiostats with an integrated lock-in amplifier (μ-Autolab, Eco Chemie, Utrecht, Netherlands). Both potentiostats were equipped with a 663 VA stand and IME interface (Metrohm). As the working electrode, a multimode Hg electrode (MME) in the state of a static Hg drop electrode (SMDE) was used. In all measurements, the reference electrode was Ag|AgCl (3M KCl, Metrohm), and a graphite electrode served as the auxiliary electrode. All measurements were carried out in a 10 mL glass electrochemical cell in a standard electrolyte solution of 0.55 M NaCl with accumulation and stirring (15–120 s) at the initial potential of −0.6 V. The amplitude of the AC voltage was 10 mV, and the optimized frequency was 77.35 Hz. The frequency was determined based on the optimization described in detail below.

All measurement data were collected following each electrochemical experiment. Each experiment was repeated three times to ensure accuracy and reproducibility. The average of these repeated measurements was taken as the representative value. The average relative standard deviation between consecutive measurements was approximately ±2 %. A surrogate SAS, i.e., Triton X-100 (TX-100), was used to quantify and characterize the adsorption-desorption effect at the Hg electrode. The calibration was carried out on both types of instruments, i.e., with and without integrated lock-in amplifier. NOVA 2.1.5 and GPES software were used to control potentiostats and data processing. The EIS measurements were carried out using a PalmSens4 instrument in combination with the PSTrace 5.8 software.

Real environmental samples with different complex matrices, including atmospheric aerosol water extracts and seawater samples, were measured to study the suitability of a newly developed electrochemical methodology.

All commercial reagents were of analytical grade. All aqueous solutions were prepared using ultrapure water (18.2 MΩ cm) at 298 K (Milli-Q, Millipore, Corp., Marlborough, USA).

3. Results and discussion

To investigate the adsorption-desorption effect and to quantify the equivalent amount of neutral SAS with AC voltammetry, the change in capacitive current was measured at a selected potential of −0.6 V after a set accumulation time. This potential is in proximity to the potential of zero charge (p.z.c.) for the system consisting of a Hg electrode in 0.55 M NaCl [6,25]. It is known that the surface coverage and the change in capacitive current relative to the current of the blank electrolyte for a set accumulation time is a function of the SAS concentration present in the solution [25]. Adsorption of SAS on the electrode surface causes a decrease in the double-layer capacitance in two ways: by (i) reducing the active surface of the equivalent capacitor and (ii) increasing the distance between the plates of the equivalent capacitor, depending on the nature of the molecules (chain length). Thus, the decrease in the capacitive current, representing the double-layer capacitance, can be interpreted as a measurement of the adsorption-desorption process [25–29]. Furthermore, qualitative information about the adsorption-desorption process can be attained by a potential scan starting from the p.z.c. in a particular direction. More details about this PSACV method can be found in the literature. [23,30–33]

Measuring the decrease of capacitive current at a set potential around p.z.c. with a potentiostat with an integrated lock-in amplifier is relatively straightforward. The angle between voltage and the AC output value can be defined, and by setting the angle to 90°, the lock-in amplifier amplifies only the capacitive current and suppresses the faradaic current [25]. Such an approach using a phase sensitivity module results in a favorable sensitivity for the non-faradaic signal. In Fig. 1A and B, the voltammograms for different additions of TX-100 are shown, as recorded by potentiostats without and with an integrated lock-in amplifier, respectively. It can be seen that the capacitive current at potential −0.6 V decreases with each addition of TX-100 until saturation occurs at the surface of the Hg electrode, corresponding to the concentration of 0.7 mg L^{-1}. Fig. 1C represents the apparent isotherm of TX-100 at the Hg electrode. In the range of 0.015–0.7 mg L^{-1}, the signal (capacitive current) is linear with respect to the blank electrolyte, and the corresponding concentration range can be used for the quantification of the adsorption-desorption process; in this case, TX-100 was used as the calibrant [25]. The characterization of the adsorption-desorption processes can be deduced from the shapes of the AC voltammograms, as these processes are potential-dependent [34,35]. The distinct peak observed at ca. −1.6 V can be attributed to the TX-100 desorption.

Using AC voltammetry without a phase sensitivity module, it is possible to measure only the total impedance of the investigated system. Such measurements are subjected to increased noise since the output

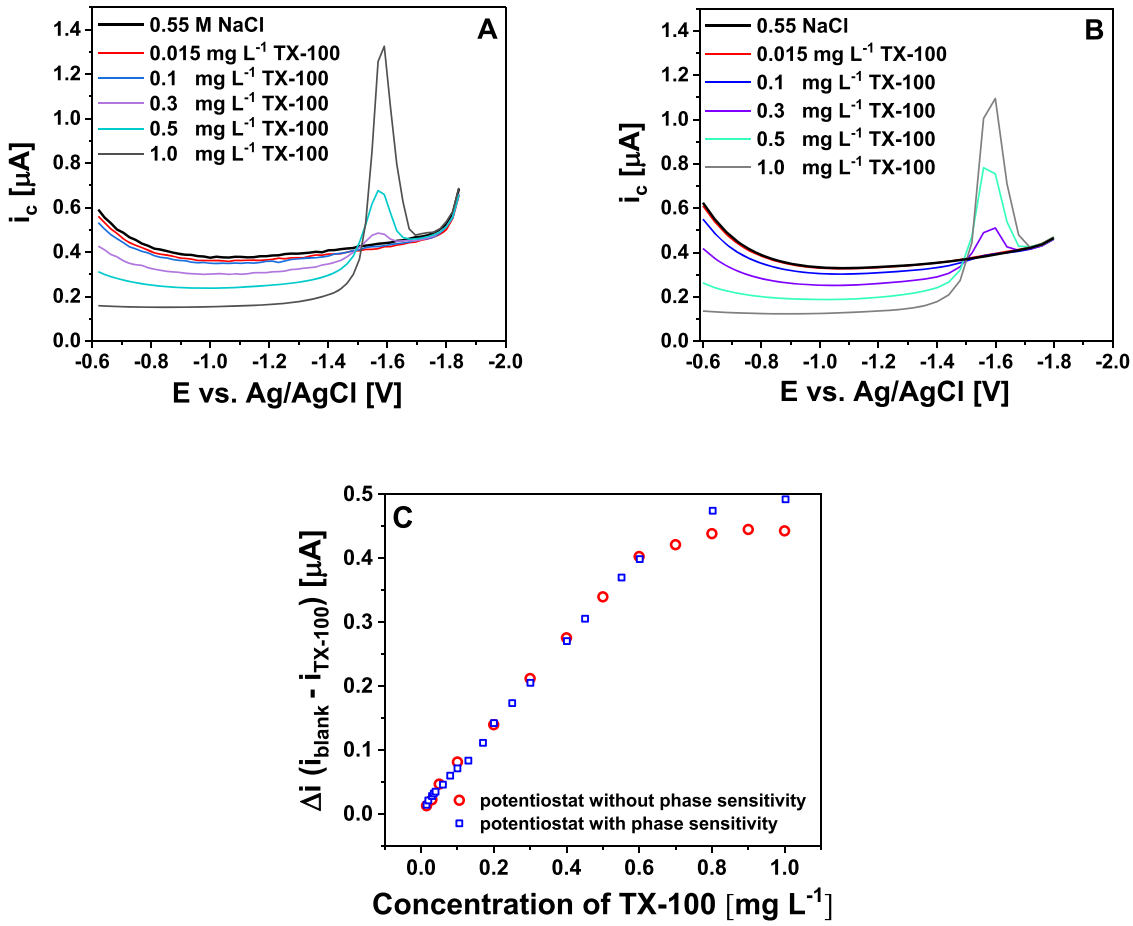

Fig. 1. AC voltammograms of TX-100 in the concentration range of 0.015–1 mg L^{-1} obtained with potentiostats A) without lock-in amplifier, B) with lock-in amplifier. C) shows apparent isotherms for TX-100 (accumulation at −0.6 V for 30 s) recorded by potentiostats without (red) and with (blue) lock-in amplifier.

signal comprises both the non-faradaic, i.e., capacitive, and faradaic currents. However, further adjustment of the AC voltammetric parameters to minimize the influence of the faradaic current is possible. In fact, AC voltammetry without a phase sensitivity module acts as a single-frequency EIS in potential scan mode. The first step in optimizing the impedance parameters is to choose the AC amplitude within the narrow linear range to avoid the effect of hysteresis [18]; the following important parameter is the selection of the excitation AC voltage frequency.

At a very high AC voltage frequency, the capacitor in Randles circuit conducts AC, exhibiting almost no impedance (resistance); thus, the imaginary component of the impedance approaches zero [2,6]. On the other hand, at a low AC voltage frequency, the capacitor behaves as a break in the equivalent electrical circuit, producing a very high impedance. In this case, all the AC flows predominantly through the parallel resistor, yielding only the faradaic current component [6]. Therefore, neither of these two extreme frequency conditions can express the capacitive current from the given equivalent circuit (see Figure S1 in SI). Even if the frequency of the capacitive and faradaic currents are identical, they can only be separated based on the difference in the phase angles. However, there should be a frequency at which the phase angle tends to increase up to 90°, indicating the dominance of non-faradaic current in the investigated system; in other words, a specific frequency should exist where the faradaic process is reduced to a minimum. EIS measurements with a frequency scan, in the range of 10, 000–1 Hz, at a potential of −0.6 V (the potential of maximum adsorption, i.e., p.z.c.), were conducted at the Hg electrode in 0.55 M NaCl containing 0.5 mg L^{-1} TX-100 to determine an optimal excitation AC voltage frequency. The corresponding data are presented in the Bode plot (Fig. 2). This narrow frequency range was selected after optimization. It was observed that below 1 Hz, the phase angle drops below 20°, indicating faradaic processes. Similarly, for frequencies above 10,000 Hz, the phase angle also decreases below 20°, further suggesting the dominance of faradaic processes.

Notably, the maximum value of the phase angle is practically inde-

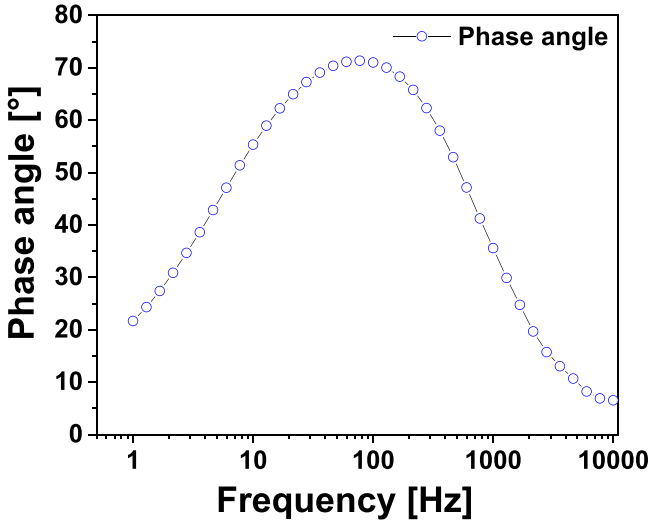

Fig. 2. Dependence of phase angle on AC frequency for Hg electrode in 0.55 M NaCl solution with the addition of 0.5 mg L^{-1} TX-100, at the potential −0.6 V.

pendent of the TX-100 concentration and the accumulation time (data not shown). However, the phase angle decreases when the set potential approaches more negative values, i.e., −1.9 V, where hydrogen evolution commences, reflecting the faradaic process (see Table 1). Fig. 2 shows that the phase angle decreases in the 10 - 1 Hz frequency range, falling between 50 and 20°. The theory states that the faradaic process is most pronounced in this range of phase angles. At a phase angle of 45°, the capacitive current is reduced by a factor of $\frac{\sqrt{2}}{2}$, thus increasing the ratio of $i_{\text{faradaic}}/i_{\text{non-faradaic}}$ and contributing to the sensitivity of the faradaic process [18]. The same is true for the 10,000 – 400 Hz frequency range. On the other hand, in the frequency range of 30 to 200 Hz, the phase angle increases to values between 70 and 73°, reaching the maximum at 77.35 Hz. From the AC capacitor circuit theory, it is known that at a phase angle of 90°, the faradaic current is reduced by a factor of $\frac{\sqrt{2}}{2}$, reducing the ratio of $i_{\text{faradaic}}/i_{\text{non-faradaic}}$ and enhancing the sensitivity towards the non-faradaic, i.e., capacitive current [18]. Explicitly, in this case (Fig. 2), the EIS measurement shows that the frequency of 77.35 Hz is optimal for extracting the non-faradaic current in an efficient manner.

Importantly, applying AC voltage in higher harmonics can result in a rise of faradaic current and a decreased phase angle[18]; thus, during this AC voltammetric methodology, the corresponding response should be recorded at the same optimal frequency.

To examine the theoretical assumption and the optimized instrumental parameters obtained by EIS, we revisit Fig. 1. It is evident that the pattern of AC decrease in both voltammograms recorded at −0.6 V (p.z.c.) by potentiostats without and with an integrated lock-in amplifier (Fig. 1A and B), respectively, are similar. To quantitatively compare the measurements obtained at the two different electrochemical instruments, the corresponding apparent isotherms were correlated; Fig. 1C shows that the linear segments of both isotherms fall within the same range. Also, the slope and intercept of the linear regions of both isotherms are practically identical (red circles: slope = 0.603, intercept = 0.0034; blue squares: slope = 0.656, intercept = 0.0067). To further demonstrate the applicability of the electrochemical methodology without a phase sensitivity module, i.e., without an integrated lock-in amplifier, and to provide insight into the influence of different complex matrices on the non-faradaic current, a set of different samples, such as seawater samples and atmospheric aerosol water extract samples, were measured in parallel by both potentiostats. The linear part of the apparent isotherm for TX-100 was used to quantify the SAS in seawater and aerosol water extract samples. The surfactant activity of these real samples is expressed as an equivalent adsorption effect of a certain amount of TX-100, as defined previously in the literature [25]. In this context, Fig. 3 shows the surface activity expressed as equivalents of TX-100 in different sample matrices, i.e., A) in seawater samples and B) in aerosol water extracts. On the x-axis, the surface activities measured with the reference method, i.e., with a PSACV, are displayed, whereas, on the y-axis, the surface activities measured without a phase sensitivity potentiostat are shown.

Table 1
AC voltammetry output data using potentiostats without lock-in amplifier for 0.5 mg L⁻[1] TX-100 in 0.55 M NaCl at the optimal frequency of 77.35 Hz.

E [V]	Z' [kΩ]	Z'' [kΩ]	|Z| [kΩ]	AC' [μA]	AC'' [μA]	|AC| [μA]	Φ [°]	Q [μC]
−0.60	1.06	21.74	21.77	0.02	0.46	0.46	87.20	0
−0.70	1.36	26.55	26.58	0.02	0.38	0.38	87.06	−0.12
−0.80	1.77	29.74	29.80	0.02	0.34	0.34	86.59	−0.25
−0.90	2.26	31.60	31.68	0.02	0.31	0.32	85.92	−0.40
−1.00	2.52	32.34	32.44	0.02	0.31	0.31	85.53	−0.57
−1.10	2.38	32.25	32.34	0.02	0.31	0.31	85.78	−0.74
−1.20	1.91	31.63	31.68	0.02	0.32	0.32	86.53	−0.91
−1.30	1.52	30.63	30.67	0.02	0.33	0.33	87.15	−1.06
−1.40	1.40	28.98	29.01	0.02	0.34	0.34	87.24	−1.21
−1.50	1.57	25.83	25.87	0.02	0.39	0.39	86.52	−1.36
−1.60	1.25	25.00	25.04	0.02	0.40	0.40	87.13	−1.50
−1.70	1.23	23.84	23.87	0.02	0.42	0.42	87.04	−1.63
−1.80	4.99	15.57	16.34	0.19	0.58	0.61	72.24	−1.77
−1.90	1.40	0.68	1.55	5.79	2.82	6.44	25.97	−2.22

Notably, Fig. 3A and B suggest that the different sample matrices have no significant influence on the capacitive current obtained by the instrument without a lock-in amplifier. However, one should note that different matrices may contain various redox active species, potentially contributing to a faradaic current component that contributes to the background noise. For both matrices, the determination coefficient and the slope are approximately 0.99 and 1, respectively, indicating no significant differences in the signal obtained from the two different potentiostats. It is important to emphasize the advantages of using the new AC voltammetric methodology without a lock-in amplifier, providing single-frequency EIS-like data, which can be useful for identifying the nature of both faradaic and non-faradaic electrochemical processes. Table 1 displays the output from AC voltammetric measurements (without lock-in amplifier) of 0.5 mg L^{-1} of TX-100 in 0.55 M NaCl. The methodology reveals the real and imaginary parts of impedance and AC and their absolute values. Additionally, it allows for monitoring the charge at each potential, while the adsorption-desorption process is more accurately represented by capacitance due to its direct dependence on these processes.

Notably, the phase angle is also shown, which can be used to follow the nature of the process taking place at each potential. This advantage allows measurement control even if a redox active species is present in the sample; thus, in the case of a faradaic process, the phase angle will shift toward lower values.

As shown in Table 1, when the phase angle approaches 90°, the imaginary impedance (*Z*'') dominates, being approximately an order of magnitude higher than the real impedance component (*Z*'), indicating a non-faradaic process. This pattern is also observed between the AC imaginary (AC'') and real (AC') parts. However, the absolute values of both impedance and AC, calculated as $|Z| = \sqrt{(Z')^2 + (Z'')^2}$ and $|AC| = \sqrt{(AC')^2 + (AC'')^2}$ are determined primarily by the higher values of their respective components. This way, the impedance and AC values reported do not come from the equivalent circuit but are measured directly from the impedance bridge as a series combination of ohmic resistance and capacitance at a specific frequency. Moreover, as the phase angle decreases to lower values, such as 25°, as observed at a potential of approximately −1.9 V (Table 1) where the faradaic process (charge transfer, specifically hydrogen evolution) occurs, the impedance and AC values change. During this faradaic process, the real components (*Z*' and AC') are higher than the imaginary components (Z'' and AC''), indicating that the absolute values of *Z* and AC are predominantly defined by the real part, highlighting the dominance of the faradaic processes. With these data outcomes, it is possible to monitor the adsorption-desorption process of SAS in a more controlled way than using PSACV. For example, the peak at −1.6 V in Fig. 1 is non-faradaic, as indicated by the phase angle close to 90° (Table 1), suggesting the desorption of TX-100 rather than charge transfer.

4. Conclusion

A study and assessment of out-of-phase AC voltammetric methodology with potentiostats lacking a phase sensitivity module were conducted. It has been shown that potentiostats without an integrated lock-in amplifier are also suitable for sensitive measurements of non-faradaic processes. Through comparison, it was demonstrated that it was possible to effectively separate (or minimize) the faradaic contribution from the total impedance signal with an optimized AC frequency and amplitude, using potentiostat without an integrated lock-in amplifier. The proposed strategy encompassing potentiostat without an integrated amplifier provides reliable and comparable results for measuring SAS compared to results obtained by potentiostat with an integrated lock-in amplifier. Finally, the new electrochemical methodology was applied to measure

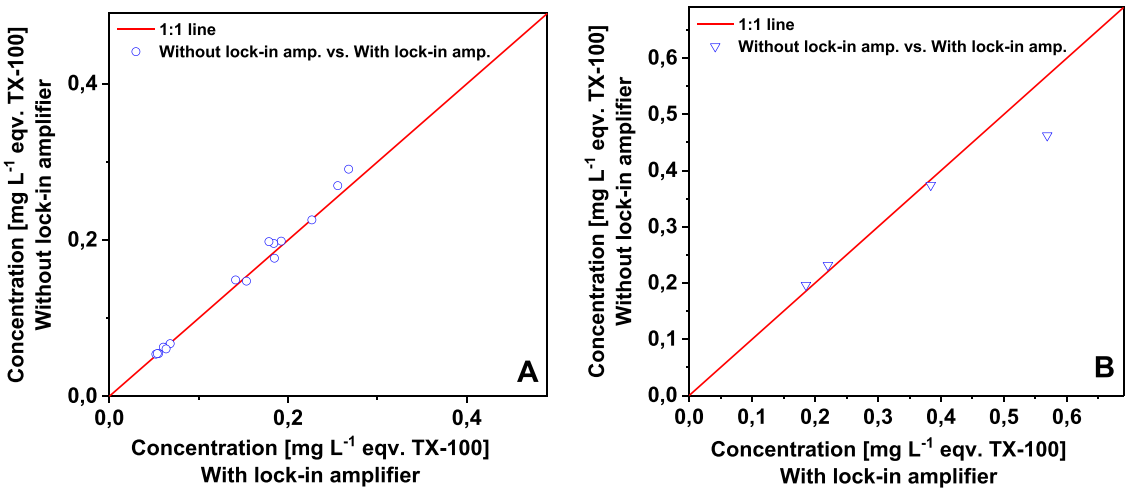

Fig. 3. Correlation between the increasing concentrations of SAS measured by potentiostats with and without lock-in amplifier for different sample matrices, i.e., A) seawater samples from Lake Rogoznica ($R^2 = 0.99$; $y = 1.06x$ - 0.005) and B) atmospheric aerosol water extract samples ($R^2 = 0.98$; $y = 0.7x + 0.08$). The red line (line 1:1) represents the scenario where the responses of the two potentiostats would be the same.

SAS in real samples, such as seawater and atmospheric aerosol water extract samples with complex matrices. This approach provides a valuable tool for conducting environmental and atmospheric studies where the involvement of SAS plays an important role and breaks down potential preconceptions about using AC voltammetry.

CRediT authorship contribution statement

Kristijan Vidović: Writing – review & editing, Writing – original draft, Methodology, Investigation, Formal analysis, Data curation, Conceptualization. **Niki Simonović:** Formal analysis. **Nikola Tasić:** Writing – review & editing. **Samo B. Hočevar:** Writing – review & editing, Funding acquisition. **Irena Ciglenečki:** Funding acquisition.

Declaration of competing interest

The authors declare that they have no known competing financial interests or personal relationships that could have appeared to influence the work reported in this paper.

Acknowledgments

This research received funding from the Slovenian Research Agency (Research Program P1–0034) and the Croatian Science Foundation project IP-2018–01–1717 (MARRES).

Supplementary materials

Supplementary material associated with this article can be found, in the online version, at doi:10.1016/j.electacta.2025.145709.

Data availability

Data will be made available on request.

References

[1] W.E. Bauer, A Voltammetric Study of the Correlations between Limiting Currents, Viscosity and Diffusion Coefficients. Ph.D. Thesis, The Pennsylvania State University, Pennsylvania, USA, 1959, pp. 1–24.
[2] H. Bauer, Alternating current polarography and tensammetry, J. Electroanal. Chem. 1 (5) (1960) 363–378, 1959.
[3] R. Muller, R. Garman, M. Droz, J. Petras, The cathode ray-tube polarograph, Ind. Eng. Chem. Anal. Ed. 10 (6) (1938) 339–341.
[4] P. Kivalo, K.K. Mustakallio. Suomen Kemistilehti B 30, 1957, p. 128.
[5] J. Boeke, H. van Suchtelen, Direkte chemische Schnellanalyse mit der Quecksilbertropfelektrode, Zeitschrift für Elektrochemie und angewandte physikalische Chemie 45 (10) (1939) 753–756.
[6] A.J. Bard, L.R. Faulkner, H.S. White. Electrochemical Methods: Fundamentals and Applications, 2nd ed., John Wiley & Sons, USA, 2022, pp. 316–340.
[7] P. Delahay, D. Turner, New instrumental methods in electrochemistry, J. Electrochem. Soc. 102 (2) (1955) 46C.
[8] H.L. Hung, D.E. Smith, Alternating current polarography with multi-step charge transfer: II. Theory for systems with quasi-reversible two-step charge transfer, J. Electroanal. Chem. 11 (6) (1966) 425–461, 1959.
[9] G. Buchanan, R. Werner, Direct current polarography in the presence of alternating voltages. II. Irreversible systems, Aust. J. Chem. 7 (4) (1954) 312–318.
[10] A.M. Bond, J. Canterford, Alternating current polarographic method of analysis in the presence of oxygen and other irreversibly reduced species, Anal. Chem. 43 (2) (1971) 228–234.
[11] Sancho, J.; Almagro, J.; Pujante, A.; Rodriguez, A., Anales Real Soc. Espan. Fis. Quim. Madrid, to be published.
[12] H.W. Nürnberg, M. von Stackelberg, Arbeitsmethoden und anwendungen der gleichspannungspolarographie: I. Apparatives, methoden und elektroden und II. Theorie der polarographischen kurve, J. Electroanal. Chem. 2 (3) (1961) 181–229, 1959.
[13] G. Jessop, In the Polarographic Determination of Aluminium, Chemistry & Industry, 1950, Soc Chemical Industry 14 Belgrave Square, London SW1X 8PS, England, 1950, pp. 560–561.
[14] J. Hayes, H. Bauer, Interpretation of the results obtained with the cambridge univector ac polarograph unit, J. Electroanal. Chem. 3 (5) (1962) 336–347, 1959.
[15] L. Balchin, D. Williams, The determination of niobium in titanium ores and pigments, Analyst 85 (1012) (1960) 503–508.
[16] K. Kishore, S.A. Akbar, Evolution of Lock-In Amplifier as Portable Sensor Interface Platform: a Review, IEEE Sens. J. 20 (18) (2020) 10345–10354.
[17] M. Meade, Advances in lock-in amplifiers, J. Phys. E: Sci. Instrum. 15 (4) (1982) 395.
[18] F. Scholz, Voltammetric techniques of analysis: the essentials, ChemTexts 1 (4) (2015) 17.
[19] B. Breyer, S. Hacobian, Tensammetry: a Method of Investigating Surface Phenomena by AC Current Measurements, Aust. J. Chem. 5 (3) (1952) 500–520.
[20] P.M. Bersier, J. Bersier, Polarographic adsorption analysis and tensammetry: toys or tools for day-to-day routine analysis? Analyst 113 (1) (1988) 3–14.
[21] P.M. Bersier, J. Bersier, Polarography, voltammetry and tensammetry: tools for day-to-day analysis in the industrial laboratory, Analyst 114 (12) (1989) 1531–1544.
[22] F.R. Simões, M.G. Xavier, 6 - Electrochemical Sensors, in: A.L. Da Róz, M. Ferreira, F. de Lima Leite, O.N. Oliveira (Eds.), Nanoscience and Its Applications, William Andrew Publishing, 2017, pp. 155–178. Eds.
[23] P. Orlović-Leko, K. Vidović, I. Ciglenečki, D. Omanović, M.D. Sikirić, I. Šimunić, Physico-chemical characterization of an urban rainwater (Zagreb, Croatia), Atmosphere (Basel) 11 (2) (2020) 144.
[24] I. Ciglenečki, P. Orlović-Leko, K. Vidović, N. Simonović, M. Marguš, J. Dautović, S. Mateša, I. Galić, The possibilities of voltammetry in the study reactivity of dissolved organic carbon (DOC) in natural waters, J. Solid State Electrochem. 27 (7) (2023) 1781–1793.
[25] B. Ćosović, V. Vojvodić, Voltammetric analysis of surface active substances in natural seawater, Electroanalysis: Int. J. Devoted Fundam. Practical Aspects Electroanalysis 10 (6) (1998) 429–434.
[26] W. Lorenz, F. Möckel, W. Müller, Zur Adsorptionsisotherme organischer Moleküle und Molekülionen an Quecksilberelektroden, I, Zeitschrift für Physikalische Chemie 25 (3_4) (1960) 145–160.

[27] R. Armstrong, W. Race, H. Thirsk, The kinetics of adsorption of neutral organic compounds at a mercury electrode, J. Electroanal. Chem. Interfacial. Electrochem. 16 (4) (1968) 517–529.
[28] B. Damaskin, A. Frumkin, A. Chizhov, Generalized model of the surface layer for the case of adsorption of organic molecules on the electrode, J. Electroanal. Chem. Interfacial. Electrochem. 28 (1) (1970) 93–104.
[29] S. Trasatti, Acquisition and analysis of fundamental parameters in the adsorption of organic substances at electrodes, J. Electroanal. Chem. Interfacial. Electrochem. 53 (3) (1974) 335–363.
[30] I. Ciglenečki, I. Vilibić, J. Dautović, V. Vojvodić, B. Ćosović, P. Zemunik, N. Dunić, H. Mihanović, Dissolved organic carbon and surface active substances in the northern Adriatic Sea: long-term trends, variability and drivers, Sci. Total Environ. 730 (2020) 139104.
[31] B. Ćosović, I. Ciglenečki, Surface active substances in the Eastern Mediterranean, Croat. Chem. Acta 70 (1) (1997) 361–371.
[32] B. Ćosović, I. Ciglenečki, D. Viličić, M. Ahel, Distribution and seasonal variability of organic matter in a small eutrophicated salt lake, Estuar. Coast. Shelf. Sci. 51 (6) (2000) 705–715.
[33] I. Ciglenečki, Z. Kodba, D. Viličić, B. Ćosović, Seasonal variation of anoxic conditions in the Rogoznica Lake, Croat. Chem. Acta 71 (2) (1998) 217–232.
[34] D. Krznarić, T. Goričnik, M. Vuković, D. Čukman, Humic acid adsorption on the Au (111) and Au polycrystalline electrode surface, Electroanalysis: Int. J. Devoted Fundam. Practical Aspects Electroanalysis 13 (2) (2001) 109–116.
[35] I. Ciglenečki, P. Orlović-Leko, K. Vidović, N. Simonović, M. Marguš, J. Dautović, S. Mateša, I. Galić, The possibilities of voltammetry in the study reactivity of dissolved organic carbon (DOC) in natural waters, J. Solid State Elect. 27 (2023) 1781–1793.